

1 Article

2 An analytical Modeling for Designing the Process 3 Parameters for Temperature Specifications in 4 Machining

5 Elham Mirkoohi ^{1*}, Peter Bocchini ², and Steven Y. Liang ¹

6 ¹ Woodruff School of Mechanical Engineering, Georgia Institute of Technology, Atlanta, GA 30332, USA;
7 steven.liang@me.gatech.edu

8 ²Boeing Research and Technology, Huntsville, AL, 35824, USA; peter.j.bocchini@boeing.com

9 * Correspondence: elham.mirkoohi@gatech.edu

10

11 **Abstract:** Different process parameters can alter the temperature during machining. Consequently,
12 selecting process parameters that lead to a desirable cutting temperature would help to increase the
13 tool life, decrease the tensile residual stress, and controls the microstructure evolution of the
14 workpiece. An inverse computational methodology is proposed to design the process parameters
15 for specific cutting temperature. A physics-based analytical model is used to predict the
16 temperature induced by cutting forces. To calculate the temperature induced by the deformation in
17 the shear zone, a moving point heat source approach is used. The shear deformation and chip
18 formation model is implemented to calculate machining forces as functions of process parameters,
19 material properties, and etc. The proposed model uses the analytical model to predict the cutting
20 temperatures and applies a variance-based recursive method to guide the inverse analysis. In order
21 to achieve the cutting process parameters, an iterative gradient search is used to adaptively
22 approach the specific temperature by the optimization of process parameters such that an inverse
23 reasoning can be achieved. Experimental data are used to illustrate the implementation and
24 validate the viability of the computational methodology.

25 **Keywords:** Inverse analysis; Temperature prediction; Process parameters; Cutting speed; Depth of
26 cut

27

28 1. Introduction

29 Temperature measurement and prediction have been a major focus of machining research for
30 several decades [1, 2]. Temperature generation during machining has a substantial effect on the tool
31 wear, tool distortion, residual stress, and microstructure evolution of the workpiece. During cutting
32 metals, a considerable amount of the input power is transferred into heat through plastic deformation
33 of the workpiece material, the friction of the chip on the tool and the friction between the tool and the
34 workpiece. The heat generated in the cutting zone can influence the cutting tool and the of the
35 workpiece qualities [3].

36 The dissipated heat can considerably change the microstructure of the workpiece. Cutting
37 process parameters such as cutting speed, feed rate, and depth of cut have a substantial influence on
38 machining temperature. Increase in cutting temperature results in greater tensile residual stress on
39 the surface of a machined component [4]. As a result, choosing viable cutting process parameters can
40 significantly help to have a desired cutting temperature.

41 Many works have been done in determining the temperature distribution in machining. In the
42 past few decades, numerical methods, such as finite element method (FEM) is utilized for the
43 temperature prediction in machining since it provides a better understanding of the heat generation
44 in the cutting zone, resulting stresses, temperature fields, and chip formation mechanisms. Lei et al.
45 developed a thermomechanical two-dimensional FE model for the orthogonal cutting process with
46 continuous chip formation [5]. Umbrello et al. developed a FE model to predict temperature when
47 steady-state conditions were reached. Pure thermal simulation is conducted in order to determine
48 the heat transfer coefficient between tool and workpiece in steady-state condition. The obtained heat
49 transfer coefficient was used in a thermomechanical simulation for temperature prediction [6]. Özel
50 et al. developed a FE model to investigate the influence of cutting-tool edge roundness on the
51 temperature field at tool–chip and tool–workpiece interfaces [7].

52 Many researches developed analytical models to predict the temperature in machining process.
53 Komanduri et al. developed an analytical model for temperature prediction. The obtained
54 temperature is combined effects of the shear plane heat source at the primary shear zone and the
55 frictional heat source at the secondary shear zone [8]. Liang et al. developed a physics-based
56 analytical model to predict temperature distribution by considering the tool thermal properties and
57 the tool wear effects [9]. Huang et al. developed a cutting temperature model with an assumption of
58 non-uniform heat intensity and partition ratio and reported improved accuracy upon validation [10].

59 Considerable accuracy is achieved from the FEM, but computational efficiency is low. On the
60 other hand, the analytical model provides accurate results. The high computational efficiency and
61 easy implementation are the other advantages of the analytical models for the machining process
62 modeling [11, 12].

63 The process parameters need to be selected in order to achieve a desirable temperature in
64 machining. Randomly choosing the process parameters and predicting the cutting temperature
65 through analytical model or finite element analysis repeatedly is not a reasonable way to achieve a
66 desirable temperature during machining. Nowadays, most of the researchers are using the trial and
67 error method in order to have a desirable workpiece performance. This method is not only time
68 consuming, but also expensive. As a result, an inverse analysis is proposed in addition to the forward
69 analysis to identify the viable solutions of process parameters that can achieve a specific performance.

70 An inverse analysis is successfully used for identification of mechanical properties which are
71 hard to be measured in experiments [13-16]. Pujana et al. used an inverse analysis to identifies the
72 coefficients of constitutive equations of flow stress in orthogonal cutting and used finite element
73 method to evaluate the results [17]. Denkena et al used the inverse analysis to predict the
74 constitutive parameters of the Johnson-Cook's flow stress model . [18]. Chen et al. chose cutting force
75 and chip thickness as targets and optimized the inverse analysis of determining Al6063 constitutive
76 model coefficients [19]. Sampsa et al. also used the inverse analysis to predict Johnson-Cook model
77 parameters with four target performances including cutting force, tangential force, resultant force,
78 and cutting temperature [20]. Mirkoohi et al. [21] used an inverse analysis to predict the process
79 parameters in turning of Ti-6Al-4V in order to achieve a desirable cutting force.

80 There are significant works on literature on modeling of the temperature during the machining
81 process. However, the lack of enough research on selecting the viable process parameters which
82 result in a desirable temperature is noticeable. The influence of cutting process parameters on
83 temperature is profound. Therefore, a systematic approach is required to obtain these cutting process
84 parameters. Determining the process parameters to ensure resulting cutting temperature can
85 significantly help to have a desirable workpiece microstructure, and also residual stress [22].

86 In order to achieve desirable cutting temperature, it is required to select the process parameters
87 in a systematic manner. A physics-based model is used to predict the temperature. The heat comes
88 from the primary shear zone and the tertiary shear zone between tool and workpiece. An imaginary
89 moving heat source approach is used to calculate the temperature field induced by the deformation
90 in the shear zone [23] . Next, an iterative gradient search procedure is set up to adaptively approach
91 the specific temperature by the optimization of process parameters such that an inverse reasoning
92 can be achieved. An iterative gradient search based on Kalman filter identifies two process

93 parameters including depth of cut and cutting velocity and achieves the optimal solution for the
94 temperature.

95 To illustrate the implementation method and validate the viability of the proposed method,
96 experimental data are used. These data are used as a starting point for inverse analysis. The proposed
97 model achieves the closest temperature to the experimental temperature by the optimization of
98 process parameters and inversely designs the cutting process parameters such as cutting velocity and
99 depth of cut.

100 2. Approach and Methodology

101 2.1. The Forward Analysis: Temperature Modeling

102 The temperature gradient induced by the cutting process can have a significant effect on the
103 residual stress, tool wear, and microstructure evolution of the workpiece. The increased in cutting
104 temperature in machining result in greater tensile residual stress on the surface of a machined
105 component [24]. In modeling of the workpiece temperature, two heat sources are assumed to exist.
106 The first is the primary heat source generated from the shear zone [25]. The second heat source is a
107 result of rubbing between the tool and the workpiece. To calculate the temperature field induced by
108 the deformation in the shear zone, a moving heat source approach is used. The temperature rises in
109 the workpiece due to shear deformation is the combined effects of the shear heat source and moving
110 heat source [23], which can be obtained as

$$111 \Delta T_{shear}(x, z) = \frac{V_c q_s}{4\pi K a} \int_0^L e^{\frac{-(x-l_i \sin \varphi) V_c}{2a_{workpiece}}} \times$$

$$112 \left\{ \sqrt{(x - l_i \sin \varphi) + (z - l_i \cos \varphi)} + \sqrt{(x - l_i \sin \varphi) + (z + \cos \varphi)} \right\} dl_i \quad (1)$$

113 where L is the shear length, $L = \frac{t}{\sin \varphi}$, φ is the shear angle, t is undeformed chip thickness, $\varphi =$
114 $\varphi - \frac{\pi}{2}$, V_c is the cutting speed, a is the workpiece thermal diffusivity, K is workpiece thermal
115 conductivity, and K_0 is the modified second Bessel function. The average shear stress in the shear
116 zone can be approximated as

$$117 q_s = \frac{(F_c \cos \varphi - F_t \sin \varphi) V_{cut} \cos \varphi}{tw \cos(\varphi - \alpha) \csc \varphi} \quad (2)$$

118 where, F_c and F_t are the cutting forces. The cutting forces consist of chip formation and
119 plowing force which can be calculated from shear deformation and chip formation model [26]. In
120 this model, the cutting plane is considered as a thick cutting band. As a result, the effects of material
121 deformation and work hardening can be considered.

122 A moving heat source can also be used to calculate the heat generated in the rubbing zone. To
123 satisfy the insulated boundary condition on the workpiece surface, an imaginary heat source is
124 imposed as coinciding with the original rubbing heat generation. The temperature rise induced by
125 the tool-workpiece rubbing can be calculated as

$$126 \Delta T_{rubbing}(x, z) = \frac{\gamma V_c q_{rub}}{2\pi K_w a_w} \times \int_0^{CA} K_0 \exp\left(-\frac{(x-s)V_c}{2a_w} \left[\sqrt{(x-s)^2 + (z)^2} \right]\right) ds \quad (3)$$

127 where CA is the work-dead zone interface length which is calculated using slip line model [27].
128 γ is heat partition coefficient that transferred to the workpiece. According to Barber [28], the heat
129 partition coefficient could be calculated as

$$130 \gamma = \frac{\rho_w C_w \sqrt{K_w}}{\rho_w C_w \sqrt{K_w} + \rho_{tool} C_{tool} \sqrt{K_{tool}}} \quad (4)$$

131

132

133

134

135

136

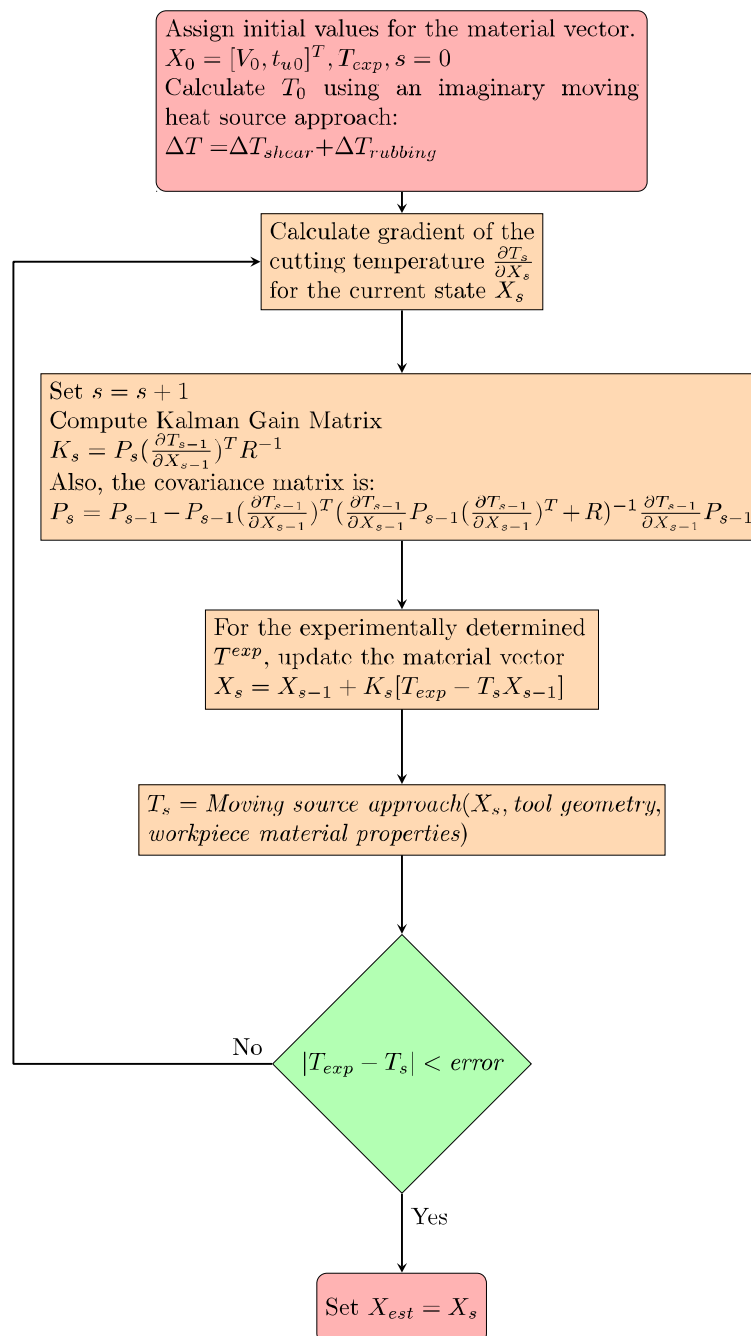
137

138 where the subscript ρ_w , C_w , and K_w are the workpiece material density, heat capacity, and
 139 thermal conductivity, respectively. ρ_{tool} , C_{tool} , and K_{tool} are corresponding the tool properties.
 140 The rubbing stress q_r is determined from the plowing force P_c in the cutting direction as

$$141 \quad q_r = \frac{P_c V_c}{w CA} \quad (5)$$

142
 143 The plowing force P_c can be calculated from traditional cutting mechanics [29], and w is the
 144 width of cut. The total temperature rise in the workpiece can be obtained by superimposing the two
 145 temperature effects from rubbing and shear as

$$146 \quad \Delta T = \Delta T_{shear} + \Delta T_{rubbing} \quad (6)$$



150

151

Figure 1. Fellow diagram of proposed inverse model

152

153 2.2. Inverse Analysis: An iterative gradient search based on Kalman filter:

154 The proposed algorithm estimates two unknown cutting process parameters which are the
 155 depth of cut (t_u) and cutting tool velocity (V) on the basis of experimentally measured cutting
 156 temperature. Fig. 1 is demonstrated the proposed approach. The two unknown constants are
 157 represented as $X = (V, t_u)^T$. At time $s = 0$, the initial estimates are $X_0 = (V_0, t_{u0})^T$. These initial
 158 estimates of cutting process parameters are used to calculate the initial cutting temperature. Then the
 159 obtained cutting temperature is compared to the desired temperature that is assigned at the first of
 160 the proposed model.

161 The estimation of subsequent cutting process parameters is obtained as

$$162 \quad X_s = X_{s-1} + K_s [T_{\text{exp}} - T_s(X_{s-1})] \quad (7)$$

163 K_s is the Kalman gain matrix, T_{exp} is the vector containing the experimentally determined
 164 temperature in machining. $T_s(X_{s-1})$ is the vector containing the cutting temperature computed from
 165 the previous iteration using forward model as explained in section 2.1.

$$166 \quad T_{\text{exp}} = [T] \quad (8)$$

$$167 \quad T_s(X_{s-1}) = [T^{s-1}] \quad (9)$$

168 The Kalman gain matrix is computed as

$$169 \quad K_s = P_s \left(\frac{\partial T_{s-1}}{\partial x_{s-1}} \right)^T R^{-1} \quad (10)$$

$$170 \quad P_s = P_{s-1} - P_{s-1} \left(\frac{\partial T_{s-1}}{\partial x_{s-1}} \right)^T \left[\left(\frac{\partial T_{s-1}}{\partial x_{s-1}} \right) P_{s-1} \left(\frac{\partial T_{s-1}}{\partial x_{s-1}} \right)^T R \right]^{-1} \times \left(\frac{\partial T_{s-1}}{\partial x_{s-1}} \right) P_{s-1} \quad (11)$$

171 The Kalman gain matrix is multiplied by the differences between the experimental and the
 172 iterated temperature to update the unknown depth of cut (t_u) and velocity (V), as shown in Eqn. 10.
 173 For the two unknown cutting process parameters (t_u and V) and the known cutting temperature, the
 174 size of the Kalman gain matrix is 2×1 . $\frac{\partial T_s}{\partial x_s} \in \mathbb{R}^{2 \times 1}$ contains the gradients of T with respect to
 175 unknown cutting process parameters. Furthermore, P_s is the simulation covariance matrix, which is
 176 the range of the unknowns at increment s , and R is the error covariance matrix, which is the size of
 177 the simulated error. P_s is updated at each step, whereas R is a non-iterative parameter that is
 178 prescribed at the initialization stage. Due to the sensitivity of the convergence rate of the Kalman
 179 algorithm to the value of P_s and R , it is essential that these two matrices be assigned properly. The
 180 initial simulation covariance matrix P_0 and the error covariance matrix R are set to be

$$181 \quad P_0 = \begin{bmatrix} \Delta V^2 & 0 \\ 0 & \Delta t_u^2 \end{bmatrix} \quad (12)$$

$$182 \quad R = [T^2] \quad (13)$$

183 where, ΔV^2 and Δt_u^2 state the predicted ranges of the unknown process parameters. In the
 184 current analysis, the diagonal components of R are chosen on the basis of the experimentally
 185 determined cutting temperature. The error threshold is used as stopping strategy for this approach.
 186 In each iteration, the error between experimental cutting temperature and predicted is computed. If
 187 the less error than the desired error is obtained, the algorithm will be terminated.

188
 189
 190
 191
 192
 193
 194
 195
 196
 197
 198
 199 **3. Results and Discussion**

In order to illustrate the implementation and also to validate the viability of the computational methodology, the orthogonal experimental data are selected from Umbrello et. al. [6]. Two chromel/alumel thermocouples (K-Type) with a diameter of 0.5 mm are embedded in the tool. The temperatures are acquired by an analogical/digital converter. The material in these experiments is AISI 1045 steel. The material properties of AISI 1045 steel is listed in Table 1 [24]. The cutting speed ranging from 50 to 100 m/min. Three different values of depth of cut (0.05, 0.1, 0.15 mm/rev) are used. The rake angle is -10° . The cutting width for all the cases is 3 mm, and the clearance angle is 11° .

Table 1. Thermal and mechanical properties of AISI 1045

Density (kg/m ³)	7800
Young's modulus (GPa)	190
Thermal expansion coefficient($^\circ\text{C}^{-1}$)	11.2
Heat capacity (J/kg $\cdot^\circ\text{C}$)	470
Thermal conductivity (W/m $\cdot^\circ\text{C}$)	49.8
Poison's ratio	0.29

In each loop, both direct analysis and inverse analysis are conducted once, and the predicted temperature is compared to the experimental measurement. By varying the depth of cut, and velocity the temperature data from the experiment, and the proposed model are listed in Table 2. The proposed inverse model tries to change the process parameters in each step in the direction that the model predicts the closest temperature to the desired temperature. The predicted cutting temperature and experimental cutting temperature are plotted in Fig. 2. The experimental cutting temperatures are the desirable values. The predicted cutting temperatures tend to be higher than the experimental values. The maximum error between the experiment and model is for sample 3, which is 9.56%. The main reason for these errors comes from the gap between the analytical model and experimental measurements in the forward analysis.

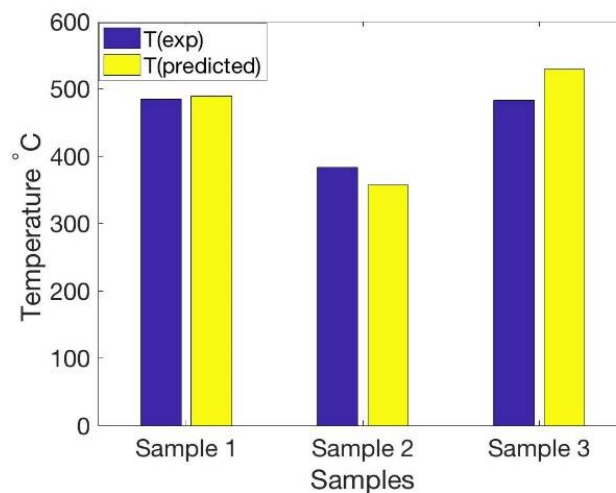
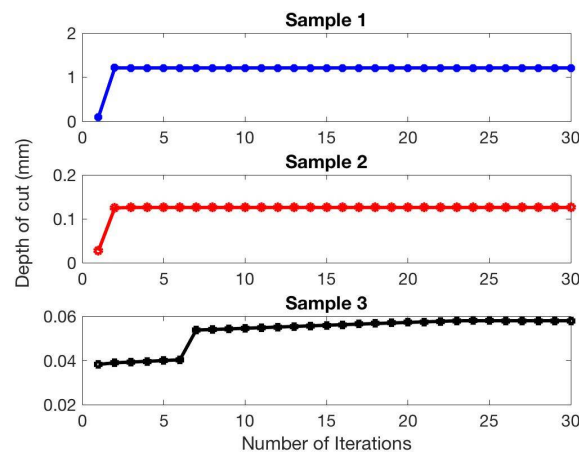


Figure 2. Comparison of predicted cutting temperature with experiments for a rake angle of -10° and different depth of cut and velocity.

Table 2. Comparison of temperature and process parameter

Samples	1	2	3
T (exp)/°C	485	383	483
T (model)/°C	489.59	357.44	529.18
V (exp)m/s	1.66	0.83	0.83
V (model)m/s	6.07	4.42	1.6
t_u (exp)/mm	0.1	0.05	0.15
t_u (model)/mm	1.2	0.12	0.058

The goal of the proposed model is to design the cutting velocity and depth of cut for a desired temperature. The initial guess $X_0 = (V_0, t_{u0})^T$ is chosen arbitrarily. For the first sample, as shown in Fig. 3 the initial depth of cut is 0.1 mm and it is converged to 1.2 mm after a very short number of iterations. This value is far from the initial specified depth of cut. The cutting velocity is plotted as a function of the number of iterations in Fig. 4. For sample 1, the initial guess is 0.5 m/s and it is converged to 6.07 m/s at a very low number of iterations, which shows the efficiency of the proposed model. This worth to note that for a given temperature, many combination of process parameters can be estimated in order to satisfy the given temperature. The cutting temperature is obtained by optimization of the process parameters, as illustrated in Fig. 5. The optimal solution for sample 1 is 489.59°C. The temperature measured from experiment is 485°C.

**Figure 3.** Evolution of depth of cut as a function of number of iterations.

For the second sample, the temperature measured from the experiments is 383 °C. This value of temperature is chosen as a desired value. The initial guess is $X_0 = [1.5, 0.05]^T$. After a very short number of iterations, it is converged to $X_s = [4.42, 0.13]^T$. The optimal predicted temperature from the proposed model is 357.44°C.

For the third sample, the temperature measured from the experiments is 483 °C. This value of temperature is also chosen as a desired value. The initial guess is $X_0 = [1.5, 0.05]^T$, and it is converged to $X_s = [1.6, 0.057]^T$. The optimal calculated temperature is 529.18°C.

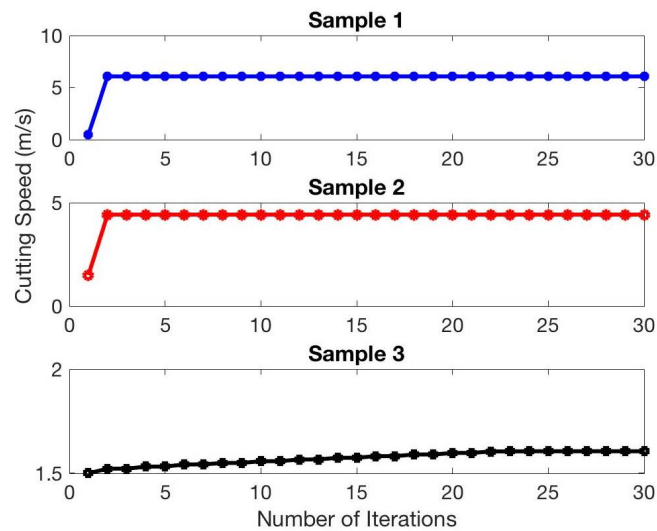


Figure 4. Evolution of cutting velocity as a function of number of iterations

273
 274
 275
 276
 277
 278
 279
 280
 281
 282
 283

By estimating the process parameters at each iteration for each sample as shown in Fig. 3 and Fig. 4 the temperature during the machining can be obtained using the forward model as explained in section 2.1. The obtained temperature is plotted as a function of number of iterations for each process parameters for all three samples as shown in Fig. 5. In sample 1 and 2, the temperature converges after two number of iterations. In sample 3 the temperature converges after eight number of iterations which shows the efficiency of the proposed model.

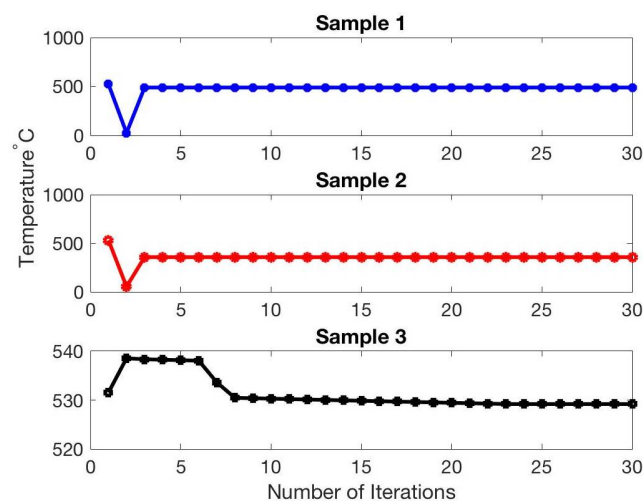


Figure 5. Evolution of temperature as a function of number of iterations

284
 285
 286
 287
 288
 289
 290
 291
 292

The shear deformation and chip formation model, as proposed by Oxley, is used to predict the cutting forces for a desirable temperature in machining. The cutting force and thrust force are plotted in Fig. 6 and Fig 7. The cutting force and thrust force follow the same trend, and they converge at very short number of iterations. The corresponding shear angle is also plotted in Fig. 8. The shear angle in these three samples has the range between 19° in sample 3 to 24° in sample 1.

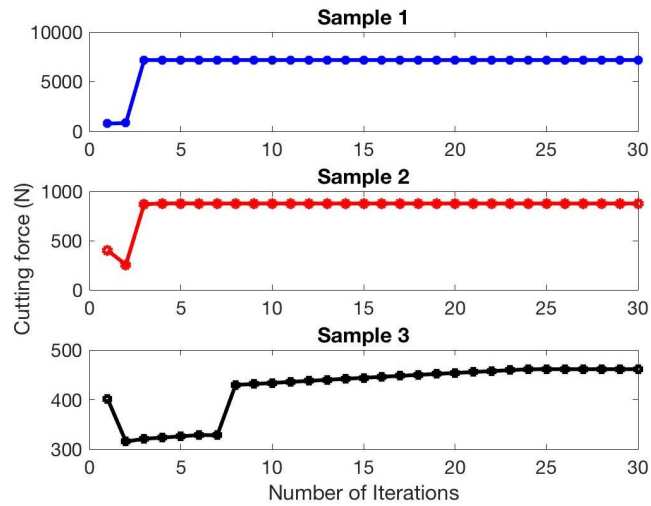


Figure 6. Evolution of cutting force as a function of number of iterations

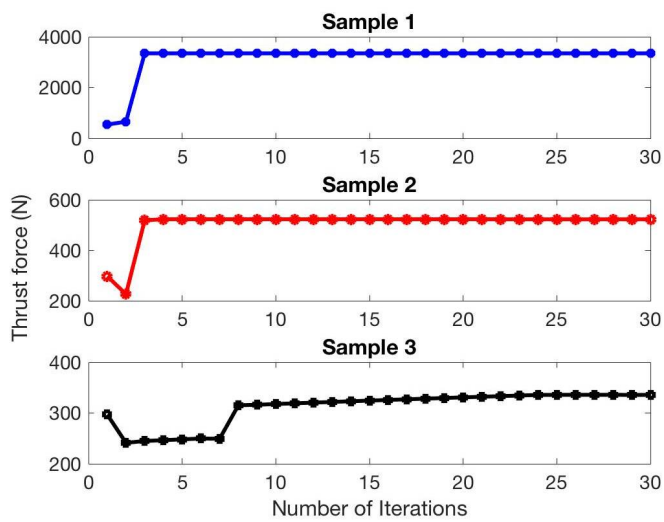


Figure 7. Evolution of cutting force as a function of number of iterations

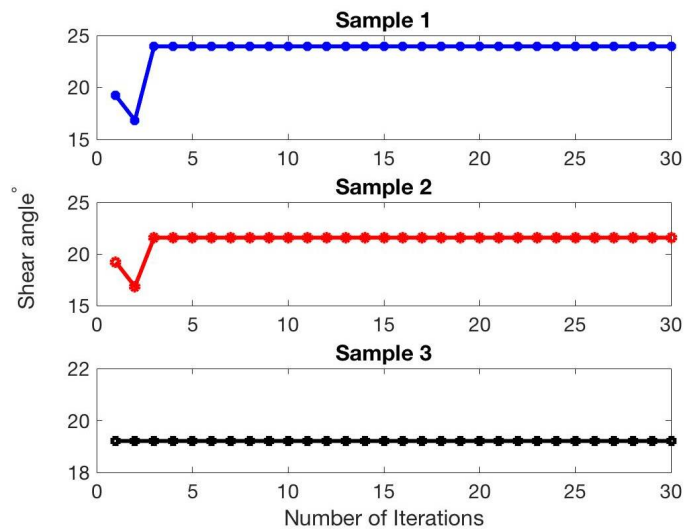


Figure 8. Evolution of shear angle as a function of number of iterations.

293
294
295
296

297
298
299
300

301
302
303
304

305 4. Conclusions

306 A physics-based model along with an iterative gradient search based on Kalman filter algorithm
307 is utilized to determine the cutting process parameters for the desired temperature. Having a
308 desirable temperature in the machining process can significantly reduce the tensile residual stress,
309 tool wear, and it helps to control the microstructure evolution of the workpiece.

310 In order to obtain the desirable cutting temperature, the viable cutting process parameters
311 should be selected. A physics-based model is used to obtain the cutting temperature using an
312 imaginary heat source approach.

313 The gradient search procedure is set up to adaptively approach the cutting temperature by the
314 optimization of process parameters such that an inverse reasoning can be achieved. Experimental
315 data are used to illustrate the implementation and also validate the viability of the computational
316 methodology.

317 The predicted cutting temperature is considerably close to the experimental data. The obtained
318 cutting process parameters are far from the initial assigned process parameters. In other words, the
319 proposed model can obtain the process parameters even when the initial guess is far from the
320 solution. The cutting velocity and depth of cut are converged at a very short number of iterations
321 which shows the efficiency of the proposed model.

322 In each iterative step, a new cutting force, and thrust force are generated which was calculated
323 using shear deformation and chip formation model for a given cutting temperature. Moreover, the
324 shear angle is obtained using an iterative algorithm. The proposed analytical model provides a fast
325 computation of process parameters for a specific temperature without needing costly experiments,
326 and time consuming finite element analysis. Furthermore, selecting viable cutting process parameters
327 which results in a specific cutting temperature, can significantly influence the tool wear, input power,
328 and also can lead to having a desirable microstructure.

329 **Author Contributions:** E.M. conceived and developed the proposed analytical model, extracted and
330 analyzed the data, and wrote the paper. P.B provided general guidance. S.Y.L. provided general
331 guidance and proofread the manuscript writing.

332 **Conflicts of Interest:** The authors declare no conflict of interest.

333 References

- 334 1. Yen, Y.-C., A. Jain, and T. Altan, A finite element analysis of orthogonal machining using different tool
335 edge geometries. *Journal of materials processing technology*, 2004. 146(1): p. 72-81.
- 336 2. Sutter, G., et al., An experimental technique for the measurement of temperature fields for the orthogonal
337 cutting in high speed machining. *International Journal of Machine Tools and Manufacture*, 2003. 43(7): p.
338 671-678.
- 339 3. Ng, E.-G., et al., Modelling of temperature and forces when orthogonally machining hardened steel.
340 *International Journal of Machine Tools and Manufacture*, 1999. 39(6): p. 885-903.
- 341 4. Thiele, J.D., et al., Effect of cutting-edge geometry and workpiece hardness on surface residual stresses in
342 finish hard turning of AISI 52100 steel. *Journal of Manufacturing Science and Engineering*, 2000. 122(4): p.
343 642-649.
- 344 5. Lei, S., Y. Shin, and F. Incropera, Thermo-mechanical modeling of orthogonal machining process by finite
345 element analysis. *International Journal of Machine Tools and Manufacture*, 1999. 39(5): p. 731-750.
- 346 6. Umbrello, D., et al., On the effectiveness of finite element simulation of orthogonal cutting with particular
347 reference to temperature prediction. *Journal of Materials Processing Technology*, 2007. 189(1-3): p. 284-291.
- 348 7. Özel, T. and E. Zeren, Finite element modeling the influence of edge roundness on the stress and
349 temperature fields induced by high-speed machining. *The International Journal of Advanced
350 Manufacturing Technology*, 2007. 35(3-4): p. 255-267.
- 351 8. Komanduri, R. and Z.B. Hou, Thermal modeling of the metal cutting process—Part III: temperature rise
352 distribution due to the combined effects of shear plane heat source and the tool–chip interface frictional
353 heat source. *International Journal of Mechanical Sciences*, 2001. 43(1): p. 89-107.
- 354 9. Li, K.-M. and S.Y. Liang, Modeling of cutting forces in near dry machining under tool wear effect.
355 *International Journal of Machine Tools and Manufacture*, 2007. 47(7-8): p. 1292-1301.

- 356 10. Huang, Y. and S. Liang, cutting forces modeling considering the effect of tool thermal property—
357 application to CBN hard turning. *International journal of machine tools and manufacture*, 2003. 43(3): p.
358 307-315.
- 359 11. Shao, Y., et al., Physics-based analysis of minimum quantity lubrication grinding. *International Journal of*
360 *Advanced Manufacturing Technology*, 2015. 79.
- 361 12. Karpat, Y. and T. Özel, Predictive analytical and thermal modeling of orthogonal cutting process—part I:
362 predictions of tool forces, stresses, and temperature distributions. *Journal of manufacturing science and*
363 *engineering*, 2006. 128(2): p. 435-444.
- 364 13. AOKI, H., et al., Use of alternative protein sources as substitutes for fish meal in red sea bream diets.
365 *Aquaculture Science*, 1997. 45(1): p. 131-139.
- 366 14. Bocciarelli, M., G. Bolzon, and G. Maier, Parameter identification in anisotropic elastoplasticity by
367 indentation and imprint mapping. *Mechanics of Materials*, 2005. 37(8): p. 855-868.
- 368 15. Nakamura, E.F., A.A. Loureiro, and A.C. Frery, Information fusion for wireless sensor networks: Methods,
369 models, and classifications. *ACM Computing Surveys (CSUR)*, 2007. 39(3): p. 9.
- 370 16. Delalleau, A., et al., Characterization of the mechanical properties of skin by inverse analysis combined
371 with the indentation test. *Journal of biomechanics*, 2006. 39(9): p. 1603-1610.
- 372 17. Pujana, J., et al., Analysis of the inverse identification of constitutive equations applied in orthogonal
373 cutting process. *International Journal of Machine Tools and Manufacture*, 2007. 47(14): p. 2153-2161.
- 374 18. Denkena, B., et al., Inverse determination of constitutive equations and cutting force modelling for complex
375 tools using oxley's predictive machining theory. *Procedia CIRP*, 2015. 31: p. 405-410.
- 376 19. Chen, X., et al., Determining Al6063 constitutive model for cutting simulation by inverse identification
377 method. *The International Journal of Advanced Manufacturing Technology*, 2017: p. 1-8.
- 378 20. Laakso, S.V. and E. Niemi, Using FEM simulations of cutting for evaluating the performance of different
379 johnson cook parameter sets acquired with inverse methods. *Robotics and Computer-Integrated*
380 *Manufacturing*, 2017. 47: p. 95-101.
- 381 21. Mirkoohi, E., P. Bocchini, and S.Y. Liang, An analytical modeling for process parameter planning in the
382 machining of Ti-6Al-4V for force specifications using an inverse analysis. *The International Journal of*
383 *Advanced Manufacturing Technology*, 2018: p. 1-9.
- 384 22. Sridhar, B., et al., Effect of machining parameters and heat treatment on the residual stress distribution in
385 titanium alloy IMI-834. *Journal of Materials Processing Technology*, 2003. 139(1-3): p. 628-634.
- 386 23. Komanduri, R. and Z.B. Hou, Thermal modeling of the metal cutting process: Part I—Temperature rise
387 distribution due to shear plane heat source. *International Journal of Mechanical Sciences*, 2000. 42(9): p.
388 1715-1752.
- 389 24. Lin, Z.-C., Y.-Y. Lin, and C. Liu, Effect of thermal load and mechanical load on the residual stress of a
390 machined workpiece. *International Journal of Mechanical Sciences*, 1991. 33(4): p. 263-278.
- 391 25. Trigger, K., An analytical evaluation of metal-cutting temperatures. *Trans. ASME*, 1951. 73: p. 57.
- 392 26. Oxley, P.L.B., *The Mechanics of Machining: An Analytical Approach to Assessing Machinability*. 1989: Ellis
393 Horwood.
- 394 27. Waldorf, D.J., R.E. DeVor, and S.G. Kapoor, A slip-line field for ploughing during orthogonal cutting.
395 *Journal of Manufacturing Science and Engineering*, 1998. 120(4): p. 693-699.
- 396 28. Sekhon, G. and J. Chenot, Numerical simulation of continuous chip formation during non-steady
397 orthogonal cutting. *Engineering computations*, 1993. 10(1): p. 31-48.
- 398 29. Waldorf, D.J., A simplified model for ploughing forces in turning. *Journal of manufacturing processes*,
399 2006. 8(2): p. 76-82.
- 400